JACS
JOURNAL OF THE AMERICAN CHEMICAL SOCIETY
Communication
pubs.acs.org/JACS

Understanding the Radical Nature of an Oxidized Ruthenium Tris(thiolate) Complex and Its Role in the Chemistry

Hao Tang, Jia Guan, and Michael B. Hall*

Department of Chemistry, Texas A&M University, College Station, Texas 77845, United States

Supporting Information

ABSTRACT: The spectroscopically observable tris(thiolate) complex $[Ru(dppbt)_3]^+$ ($\mathbf{1}^+$) (dppbt = diphenylphosphinobenzenethiolate) is reported to have chemistry based on thiyl-radical character. High-level *ab initio* methods predict the ground-state electronic structure of $\mathbf{1}^+$ to be an open-shell diradical singlet state with antiferromagnetic coupling between (S = 1/2) Ru(III) and (S = 1/2) S p_z, rather the previous description based on a diradical state involving two S p orbitals. These new results provide an improved understanding of the experimental chemistry of $\mathbf{1}^+$ and related species.

Recently, interest in non-innocent ligands has expanded dramatically, and dithiolenes have played a key role in understanding such ligands.[1,2] Following Schrauzer,[3] Wing,[4] and their co-workers, who reported high reactivity of dithiolene complexes toward strained and cyclic alkenes, Wang and Stiefel applied nickel dithiolene complexes as electrochemical catalysts for separation of olefins from a feedstock.[5] Recent experimental and computational studies have finally elucidated the mechanistic details of these and related metal dithiolenes.[6,7]

The chelating ligand diphenylphosphinobenzenethiolate (dppbt), initially reported by Dilworth et al.,[8] has the ability to delocalize electron density like dithiolenes. Recently, Grapperhaus and co-workers synthesized the tris(thiolate) complexes $[Ru(dppbt)_3]^n$ ($\mathbf{1}^n$, n = −, 0, +), and demonstrated that $\mathbf{1}^+$ readily undergoes addition reactions with a variety of unsaturated organic compounds.[9]

Using density functional theory (DFT), these workers[9g] examined the electronic structure of $\mathbf{1}^n$, for which a schematic MO diagram is shown in Figure 1. The π_{xz}/π^*_{xz} are the bonding/antibonding MOs between Ru-d_{xz} and the in-phase combination of the S2-p_z and S3-p_x orbitals. Similarly, the π_{yz}/π^*_{yz} are bonding/antibonding MOs of the Ru-d_{yz} and the coplanar S1-p_y orbital, and are essentially orthogonal to the pair in the other plane.

The totally reduced species, $\mathbf{1}^-$, is best described as Ru(II) with three anionic S ligands. Because of the near degeneracy of the π^*_{yz} and π^*_{xz} orbitals, oxidation of $\mathbf{1}^-$ by two electrons poses a dilemma for the electronic configuration of $\mathbf{1}^+$ (Figure 1). For the closed-shell (CS) singlet state, $^1\mathbf{A}$, the highest occupied MO (HOMO) and lowest unoccupied MO (LUMO) are the π^*_{yz} orbital and π^*_{xz} orbital, respectively (Figure 1a). Alternatively, spin-unrestricted solutions could result in the "broken-symmetry" open-shell (OS) singlet, $^1\mathbf{B}$, (Figure 1b) or the triplet state, $^3\mathbf{C}$, (Figure 1c). In magnetic language, these

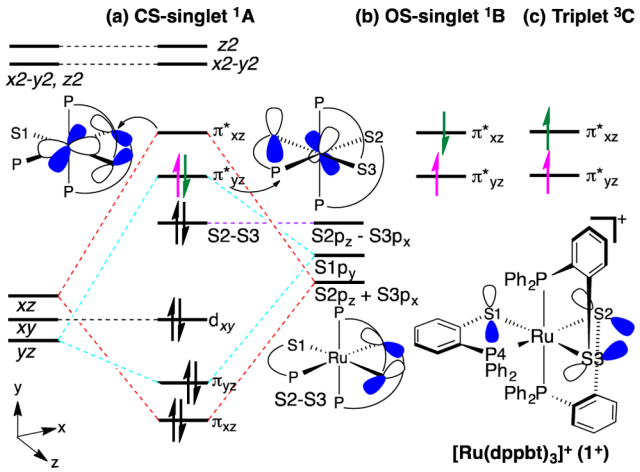

Figure 1. In this schematic MO diagram for $\mathbf{1}^n$ (n = −, 0, +), $\mathbf{1}^-$ has the π^*_{xz} filled, $\mathbf{1}^0$ has 1e$^-$ in this orbital, while $\mathbf{1}^+$ has three possible occupation schemes: (a), (b), and (c).

two states have unpaired electrons in the π^*_{xz} and π^*_{yz} orbitals, antiferromagnetically coupled in $^1\mathbf{B}$ but ferromagnetically coupled in $^3\mathbf{C}$.

The previous DFT calculations on $\mathbf{1}^+$ predicted that $^3\mathbf{C}$ was more stable than the $^1\mathbf{A}$ by 1.3 kcal/mol, while experimentally $\mathbf{1}^+$ was diamagnetic; thus, Grapperhaus and co-workers proposed a "singlet diradical", like $^1\mathbf{B}$, as the ground state because of the "nearly degenerate electronic ground state".[9g] Although S1 has the highest spin density based on the triplet-state calculations, it was ruled out as the reactive radical site because this assignment would be inconsistent with the observed reactivity. Thus, they proposed an electronic ground state "akin to the generally accepted ground state of ozone", a spin-paired (t_{2g}-like) "Ru(II) dithiyl radical" with the diradical localized on two sulfurs, S2 and S3.[9b,g] The thiyl radical nature of $\mathbf{1}^+$ was further verified by the chemical reactivity studies that gave some support to "the ozone model" by the participation of S3 and S2 in radical-like chemistry.[9h]

Grapperhaus and co-workers did not report detailed calculations of this open-shell diradical state, and in our hands this state, $^1\mathbf{B}$, is higher in energy than either the CS singlet, $^1\mathbf{A}$, or the triplet state, $^3\mathbf{C}$ (as might be expected for the orbitals' orthogonality, see free-energy differences in Figure 2). Although $\mathbf{1}^+$ clearly displays chemistry corresponding to having

Received: September 2, 2015
Published: November 22, 2015

DOI: 10.1021/jacs.5b09309
J. Am. Chem. Soc. 2015, 137, 15616−15619

thiyl radical character, an accurate picture of its ground-state electronic structure is still elusive.

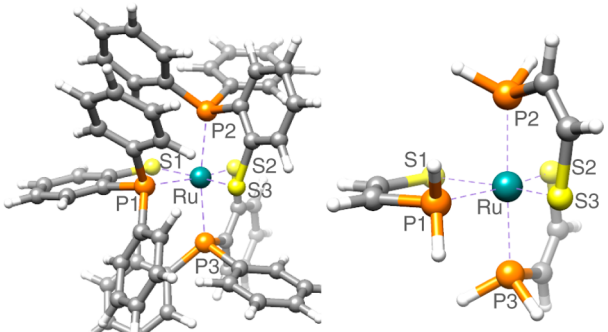

a) 1^+ (^{1}A/^{1}B/^{3}C)		b) 2^+ (^{1}A/^{1}B/^{3}C)	
	ΔG 2.3/2.8/0.0		ΔG 0.9/2.2/0.0
Ru-S1	2.46/2.29/2.29	Ru-S1	2.45/2.31/2.30
Ru-S2	2.24/2.32/2.32	Ru-S2	2.24/2.31/2.31
Ru-S3	2.23/2.35/2.36	Ru-S3	2.26/2.37/2.37
Ru-P1	2.45/2.42/2.43	Ru-P1	2.40/2.35/2.36
Ru-P2	2.41/2.42/2.42	Ru-P2	2.34/2.36/2.37
Ru-P3	2.43/2.44/2.44	Ru-P3	2.36/2.36/2.37

Figure 2. DFT(ω-B97XD)-optimized geometries are given with the bond lengths (Å) for (a) the full model $\mathbf{1}^+$ and (b) the truncated model $\mathbf{2}^+$. Relative free energies with solvent corrections are in kcal/mol.

To produce a complete description of the electronic structure and radical character of $\mathbf{1}^+$, we employed a series of high-level *ab initio* methods: CASSCF, CASPT2, MP2, MP3, MP4D, MP4DQ, CCSD, QCISD, QCISD(T), and CCSD(T). DFT calculations were also performed with a variety of functionals: BP86, M06, TPSS, B97D, TPSSh, ω-B97XD, B3LYP, MN12SX, BMK, and BHandHLYP. Geometries and frequencies were computed with the mixed basis set (SDD(f)(Ru)/6-311G*(C, P, S, and H) and 6-31G(C and H on Ph)). Single-point calculations were computed with the SDD(f)(Ru)/6-311++G**(rest) basis set. All the functionals converged smoothly to the CS-singlet, ^{1}**A**, and triplet state, ^{3}**C**, but the symmetry-broken OS-singlet state, ^{1}**B**, could only be obtained with ω-B97XD, attempts to converge the ^{1}**B** state with other functionals always resulted in convergence to the ^{1}**A**. Because ω-B97XD also predicted geometries for $\mathbf{1}^-$ that agreed with the experimental values (Table S4), all the DFT results reported in the main text are those from ω-B97XD calculations (see Supporting Information (SI) for other functionals). Calculations were carried out with the Gaussian 09[10] and MOLPRO[11] program packages (details in SI).

To save computational cost for the high-level *ab initio* calculations on $\mathbf{1}^+$, we employed a truncated model $\mathbf{2}^+$ (Figure 2b) that mimics the coordination sphere of Ru as much as possible. As shown in Figure 2, the geometric agreement for the full and truncated model structures of the singlet (^{1}**A** and ^{1}**B**) and triplet (^{3}**C**) states is satisfying (Ru−S and Ru−P bond lengths differ by ≤0.03 and ≤0.08 Å, respectively). Furthermore, the calculated metal−ligand bond distances of the full and truncated molecules reproduce the experimental values for $\mathbf{1}^-$ within ≤0.04 ($\mathbf{1}^-$) and ≤0.05 Å ($\mathbf{2}^-$), and the truncated model reproduces the various trans influences seen in the full model for the different electronic states (Figure 2 and Table S7). Moreover, the free-energy trend at the ω-B97XD/SDD(f)(Ru) and 6-311++G**(rest)//ω-B97XD/SDD(f)(Ru) and 6-311G*(rest) level from the highest to lowest energy: ^{1}**B**, ^{1}**A**, and ^{3}**C** shows good agreement between the full and truncated models (Figure 2). In addition, by visual inspection the relevant Kohn−Sham orbitals of $\mathbf{2}^+$ and $\mathbf{1}^+$ (Figures S1−S6) remains essentially unchanged. Thus, the truncated model $\mathbf{2}^+$ should serve as a good model for $\mathbf{1}^+$.

To elucidate the electronic structures, we performed CASSCF(10,6) optimizations (**State′**) on the truncated model $\mathbf{2}^+$ and CASPT2 (**State″**) single-point calculations at the SDD(f) (Ru) and 6-311G*(rest) level (see Table S6 in SI). For the CASSCF the ^{1}**A′** is well represented the two configurations Ψ_1 and Ψ_2 (Scheme 1) that are related by a 2e$^-$ excitation from the bonding MO between Ru-d$_{xz}$ and S2-p$_z$ (ψ_3) to its antibonding MO (ψ_1) (Scheme 1). The strong contribution from the double excitation results in the electron occupation numbers of ψ_3 (1.65) and ψ_1 (0.35). After considering dynamic correlation from the CASPT2 calculation, the multiconfigurational character of the ^{1}**A″** is more prominent with one major configuration Φ_1 and a number of other significant contributions (Scheme 2). Now the CASPT2 orbitals, which are localized atomic-like orbitals, show that the two spin-coupled singly occupied orbitals are the Ru-d$_{xz}$ (ϕ_1) and the S2-p$_z$ (ϕ_3) with the electron occupation numbers of 1.10 and 1.08, respectively (Scheme 2). Thus, the CASPT2 ground state with localized orbitals is a singlet diradical state, but it involves antiferromagnetically coupling of a S = 1/2 Ru(III) with a S = 1/2 S2-p$_z$ (Scheme 2). The next two most important configurations Φ_2 and Φ_3 have ϕ_6 (S3-p$_x$) singly occupied; Φ_2 is the thiyl diradical (S2−S3, ozone-like), while

Scheme 1. Main Electronic Configurations (Ψ_i), Electron Occupation Numbers (Blue), Natural Orbitals (ψ_i), and Relative Energies of Singlet and Triplet States for CASSCF (^{1}A′, ^{1}B′, and ^{3}C′)

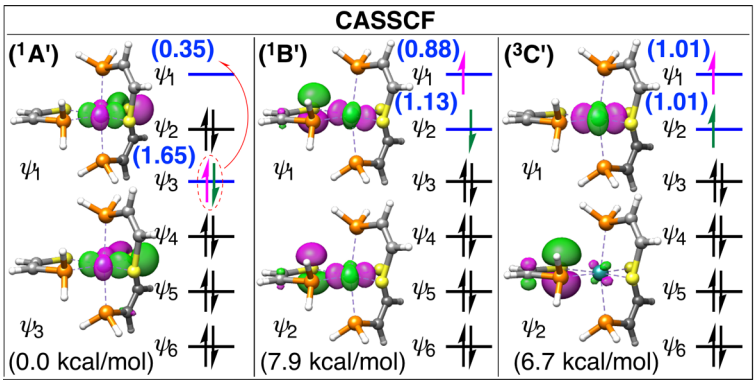

State	Configuration state function	Coeff.
^{1}A′	Ψ_1 $(\psi_1)^0(\psi_2)^2(\psi_3)^2(\psi_4)^2(\psi_5)^2(\psi_6)^2$	0.91
	Ψ_2 $(\psi_1)^2(\psi_2)^2(\psi_3)^0(\psi_4)^2(\psi_5)^2(\psi_6)^2$	-0.42
^{1}B′	Ψ_1 $(\psi_1)^0(\psi_2)^2(\psi_3)^2(\psi_4)^2(\psi_5)^2(\psi_6)^2$	0.75
	Ψ_2 $(\psi_1)^2(\psi_2)^0(\psi_3)^2(\psi_4)^2(\psi_5)^2(\psi_6)^2$	-0.66
^{3}C′	Ψ_1 $(\psi_1)^1(\psi_2)^1(\psi_3)^2(\psi_4)^2(\psi_5)^2(\psi_6)^2$	0.99
	Ψ_2 $(\psi_1)^2(\psi_2)^2(\psi_3)^2(\psi_4)^1(\psi_5)^1(\psi_6)^2$	0.10

$\Psi = \sum_i c_i \Psi_i$, ψ is the CASSCF natural orbital.

DOI: 10.1021/jacs.5b09309
J. Am. Chem. Soc. 2015, 137, 15616−15619

Scheme 2. Main Electronic Configurations (Φ_i), Electron Occupation Numbers (Blue), Localized Orbitals (ϕ_i), and Relative Energies of Singlet and Triplet States for CASPT2 (^{1}A″, ^{1}B″, and ^{3}C″)

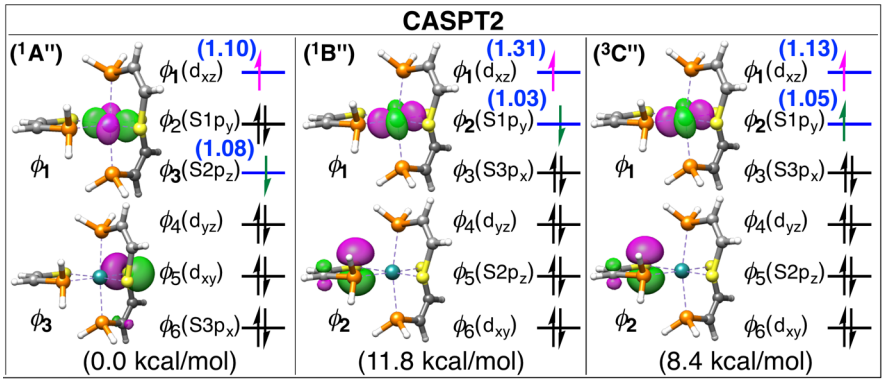

State	Configuration state function	Coeff.
^{1}A″	Φ_1 $(\phi_1)^1(\phi_2)^2(\phi_3)^1(\phi_4)^2(\phi_5)^2(\phi_6)^2$	0.86
	Φ_2 $(\phi_1)^2(\phi_2)^2(\phi_3)^1(\phi_4)^2(\phi_5)^2(\phi_6)^1$	0.27
	Φ_3 $(\phi_1)^1(\phi_2)^2(\phi_3)^2(\phi_4)^2(\phi_5)^2(\phi_6)^1$	-0.25
	Φ_4 $(\phi_1)^0(\phi_2)^2(\phi_3)^2(\phi_4)^2(\phi_5)^2(\phi_6)^2$	-0.22
	Φ_5 $(\phi_1)^2(\phi_2)^2(\phi_3)^0(\phi_4)^2(\phi_5)^2(\phi_6)^2$	-0.19
^{1}B″	Φ_1 $(\phi_1)^1(\phi_2)^1(\phi_3)^2(\phi_4)^2(\phi_5)^2(\phi_6)^2$	0.82
	Φ_2 $(\phi_1)^2(\phi_2)^1(\phi_3)^2(\phi_4)^1(\phi_5)^2(\phi_6)^2$	-0.40
^{3}C″	Φ_1 $(\phi_1)^1(\phi_2)^1(\phi_3)^2(\phi_4)^2(\phi_5)^2(\phi_6)^2$	0.92
	Φ_2 $(\phi_1)^2(\phi_2)^1(\phi_3)^1(\phi_4)^2(\phi_5)^2(\phi_6)^2$	0.25

$\Phi = \sum_i c_i \Phi_i$, ϕ is the CASPT2 localized orbital.

Φ_3 is a Ru(III) thiyl radical like Φ_1, but with S3. The next most important configurations, Φ_4 and Φ_5, are CS ones that represent Ru(II) and Ru(IV) contributions. Overall, the electronic structure is best assigned as Ru(III) (S = 1/2) antiferromagnetically coupled to S2-p$_z$ (S = 1/2), rather than either the CS-singlet with Ru(IV) (S = 0) and S2-p$_z$ (S = 0) or the other OS-singlet (dithiyl) like Ru(II) (S = 0) with S2-p$_z^\bullet$ (S = 1/2) and S3-p$_x^\bullet$ (S = 1/2).

The triplet states (^{3}**C**′ and ^{3}**C**″) at both the CASSCF and CASPT2 levels are totally dominated by one identical configuration (Schemes 1 and 2). In the CASSCF the two singly occupied orbitals, ψ_1 and ψ_2, are the Ru-d$_{xz}$ and S1-p$_y$ orbitals with electron occupation numbers of 1.01 (ψ_1) and 1.01 (ψ_2) (Scheme 1), likewise in the CASPT2 the resulting (nearly identical) orbitals ϕ_1 and ϕ_2 have electron occupation numbers of 1.13 (ϕ_1) and 1.05 (ϕ_2) (Scheme 2). Therefore, this state has a Ru(III) center (S = 1/2) coupled ferromagnetically with S1-p$_y$ (S = 1/2) (Scheme 2). *Most importantly, the true ground-state singlet and the lowest energy triple state involve different S singly occupied orbitals.*

For the OS diradical singlet state, ^{1}**B**, the CASSCF calculations show that the two key orbitals, ψ_1 and ψ_2, are delocalized MOs related to the singly occupied MOs in ^{3}**C**′; here, alternatively doubly occupied or vacant in the two main closed shells of ^{1}**B**′ (Scheme 1). The nearly equal contributions of these two configurations produce electron occupation numbers of 0.88 and 1.13 for these delocalized combinations of Ru-d$_{xz}$ (ψ_1) and S1-p$_y$ (ψ_2) orbitals. This CASSCF wave function is equivalent to one with open-shell singlet coupling between the Ru-d$_{xz}$ and S1-p$_y$ electrons (Scheme 1). After the CASPT2 calculations, the diradical character is more obviously displayed in ^{1}**B**″, where the leading configuration Φ_1 with the coefficient of 0.82 (Scheme 2) has one electron in each of these two localized orbitals and the complete CASPT2 wave function produces electron occupation numbers of 1.31 and 1.03 for Ru-d$_{xz}$ (ϕ_1) and S1-p$_y$ (ϕ_2), respectively (Scheme 2). This state ^{1}**B**″ is related to the triplet state ^{3}**C**″, since they share a similar electronic configuration (Scheme 2), but ^{1}**B**″ has antiferromagnetically coupled electrons between the S1 radical and the Ru(III) radical, while ^{3}**C**″ has these electrons ferromagnetically coupled.

Both CASSCF and CASPT2 calculations predict the ground state to be ^{1}**A**, while the ^{3}**C** state is 6.7 and 8.4 kcal/mol higher, respectively, and the ^{1}**B** state is 7.9 and 11.8 kcal/mol higher, respectively. Another triplet state based on d$_\pi$ and S2-p$_z$ is much less stable than the other three states (Figure S11 and Table S11). Thus, the open-shell singlet that was thought to be the ground state, the ^{1}**B**, is considerably higher in energy; furthermore, this ^{1}**B** state has S1 radical character, the S that does not display the radical character chemically. To gain additional predictions of the relative energies of these states, we carried out single-point calculations using various electronic structure methods at the SDD(f)(Ru) and 6-311G*(rest) level on the ω-B97XD-optimized geometries of **2**$^+$. Like the CASSCF and CASPT2 predictions, the CCSD(T) results predict a ^{1}**A** ground state with the ^{3}**C** and the ^{1}**B** states is 5.3 and 7.2 kcal/mol higher, respectively (see Table S14 for results of other single-reference methods).

In conclusion, the high-level *ab initio* calculations reported here provide an unambiguous electronic structure description of the tris(thiolate) complex **1**$^+$ that was not available from the DFT calculations. The ground state electronic structure of **1**$^+$ is a singlet diradical ground state, as previously suggested by Grapperhaus,[9g] but it is best described as an OS diradical singlet state with antiferromagnetic coupling between a d$_\pi$ electron on the Ru(III) and p$_\pi$ electron on the S2, rather the previous description based on a Ru(II)-dithiyl, a diradical state involving two S p$_\pi$ orbitals.[9g,h] This new assignment clarifies the experimental reaction of **1**$^+$ with alkenes and alkynes. Tedder's Rules[12] for radical alkene addition suggests that radical substitution should occur initially at the unsubstituted carbon; thus, the dominant radical character on S2 of **1**$^+$ is responsible for the previous findings that the position of the unsubstituted carbon of asymmetrical substrates is on S2 as opposed to S3, i.e., [**1**-*m*-methylstyrene]$^+$,[9b] [**1**-*p*-methylstyrene]$^+$,[9b] [**1**-octyne]$^+$,[9e] and [**1**-CH$_2$C(O)R]$^+$ (Scheme 3a).[9c] Equally interesting, deprotonation of the [**1**-ethylene]$^+$ produces the isomer [**1**-C$_2$H$_3$]^0 with the vinyl group on S2 rather than on S1 or S3, as observed crystallographically and computationally (Scheme

Scheme 3. Stereo- and Regioselectivity

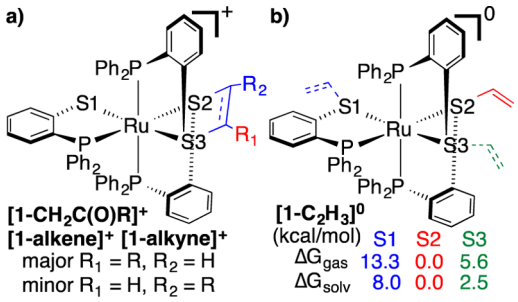

DOI: 10.1021/jacs.5b09309
J. Am. Chem. Soc. 2015, 137, 15616−15619

3b).[9i] This regioselectivity may be ascribed to higher radical character on S2, which stabilizes the vinyl group on S2 as shown by the free-energy differences in Scheme 3b. These results are also consistent with the multi-configurational ground state predicted here and with prior arguments regarding the stereo- and regio-selectivity arising from higher spin density on the S *trans* to P.[9b,c,e,i]

■ ASSOCIATED CONTENT

Supporting Information

The Supporting Information is available free of charge on the ACS Publications website at DOI: 10.1021/jacs.5b09309.

Computational details and references; Cartesian coordinates; Tables S1−S15 and Figures S1−S14, which include energies and spin densities from other functionals and larger CASSCF calculations up to CASSCF-(24,14) (PDF)

■ AUTHOR INFORMATION

Corresponding Author

*mbhall@tamu.edu

Notes

The authors declare no competing financial interest.

■ ACKNOWLEDGMENTS

We acknowledge financial support from the Qatar National Research Fund under NPRP grant 05-318-1-063. Computer time was provided by the TAMU Supercomputer Facility.

■ REFERENCES

(1) For recent reviews on non-innocence, see: (a) Eisenberg, R.; Gray, H. B. *Inorg. Chem.* **2011**, *50*, 9741. (b) Eisenberg, R. *Coord. Chem. Rev.* **2011**, *255*, 825. (c) Ray, K.; Petrenko, T.; Wieghardt, K.; Neese, F. *Dalton Trans.* **2007**, 1552. (d) Forum Issue on redox-active ligands. *Inorg. Chem.* **2011**, *50*, 9737−9914.10.1021/ic201881k (e) Forum Issue on redox-active ligands. *Eur. J. Inorg. Chem.* **2012**, *3*, 340−580.10.1002/ejic.201101359 (f) Gunanathan, C.; Milstein, D. *Science* **2013**, *341*, 1229712. (g) Luca, O. R.; Crabtree, R. H. *Chem. Soc. Rev.* **2013**, *42*, 1440. (h) Tezgerevska, T.; Alley, K. G.; Boskovic, C. *Coord. Chem. Rev.* **2014**, *268*, 23. (i) Li, H.; Hall, M. B. *ACS Catal.* **2015**, *5*, 1895.

(2) For selected studies on dithiolenes, see: (a) Gray, H. B.; Billig, E. *J. Am. Chem. Soc.* **1963**, *85*, 2019. (b) Davison, A.; Edelstein, N.; Holm, R. H.; Maki, A. H. *Inorg. Chem.* **1963**, *2*, 1227. (c) Szilagyi, R. K.; Lim, B. S.; Glaser, T.; Holm, R. H.; Hedman, B.; Hodgson, K. O.; Solomon, E. I. *J. Am. Chem. Soc.* **2003**, *125*, 9158. (d) Ray, K.; Weyhermüller, T.; Neese, F.; Wieghardt, K. *Inorg. Chem.* **2005**, *44*, 5345.

(3) For selected examples of dithiolenes addition reactions with olefins, see: (a) Schrauzer, G. N.; Mayweg, V. P. *J. Am. Chem. Soc.* **1965**, *87*, 1483. (b) Schrauzer, G. N.; Rabinowitz, H. N. *J. Am. Chem. Soc.* **1968**, *90*, 4297. (c) Schrauzer, G. N.; Ho, R. K. Y.; Murillo, R. P. *J. Am. Chem. Soc.* **1970**, *92*, 3508.

(4) (a) Wing, R. M.; Tustin, G. C.; Okamura, W. H. *J. Am. Chem. Soc.* **1970**, *92*, 1935. (b) Baker, J. R.; Hermann, A.; Wing, R. M. *J. Am. Chem. Soc.* **1971**, *93*, 6486.

(5) Wang, K.; Stiefel, E. I. *Science* **2001**, *291*, 106.

(6) For recent examples of bis(dithiolene), see: (a) Harrison, D. J.; Nguyen, N.; Lough, A. J.; Fekl, U. *J. Am. Chem. Soc.* **2006**, *128*, 11026. (b) Kerr, M. J.; Harrison, D. J.; Lough, A. J.; Fekl, U. *Inorg. Chem.* **2009**, *48*, 9043. (c) Dang, L.; Shibl, M. F.; Yang, X.; Alak, A.; Harrison, D. J.; Fekl, U.; Brothers, E. N.; Hall, M. B. *J. Am. Chem. Soc.* **2012**, *134*, 4481. (d) Dang, L.; Shibl, M. F.; Yang, X.; Harrison, D. J.; Alak, A.; Lough, A. J.; Fekl, U.; Brothers, E. N.; Hall, M. B. *Inorg. Chem.* **2013**, *52*, 3711. (e) Dang, L.; Ni, S. F.; Hall, M. B.; Brothers, E. N. *Inorg. Chem.* **2014**, *53*, 9692.

(7) For recent examples of tri(dithiolene), see: (a) Cervilla, A.; Llopis, E.; Marco, D.; Perez, F. *Inorg. Chem.* **2001**, *40*, 6525. (b) Harrison, D. J.; Lough, A. J.; Nguyen, N.; Fekl, U. *Angew. Chem., Int. Ed.* **2007**, *46*, 7644.

(8) (a) Dilworth, J. R.; Hutson, A. J.; Morton, S.; Harman, M.; Hursthouse, M. B.; Zubieta, J.; Archer, C. M.; Kelly, J. D. *Polyhedron* **1992**, *11*, 2151. (b) Dilworth, J. R.; Zheng, Y.; Lu, S.; Wu, Q. *Transition Met. Chem.* **1992**, *17*, 364.

(9) (a) Grapperhaus, C. A.; Poturovic, S. *Inorg. Chem.* **2004**, *43*, 3292. (b) Ouch, K.; Mashuta, M. S.; Grapperhaus, C. A. *Inorg. Chem.* **2011**, *50*, 9904. (c) Poturovic, S.; Grapperhaus, C. A.; Mashuta, M. S. *Angew. Chem., Int. Ed.* **2005**, *44*, 1883. (d) Grapperhaus, C. A.; Venna, K. B.; Mashuta, M. S. *Inorg. Chem.* **2007**, *46*, 8044. (e) Ouch, K.; Mashuta, M. S.; Grapperhaus, C. A. *Eur. J. Inorg. Chem.* **2012**, *2012*, 475. (f) Sampson, K. O.; Kumar, D.; Mashuta, M. S.; Grapperhaus, C. A. *Inorg. Chim. Acta* **2013**, *408*, 1. (g) Grapperhaus, C. A.; Kozlowski, P. M.; Kumar, D.; Frye, H. N.; Venna, K. B.; Poturovic, S. *Angew. Chem., Int. Ed.* **2007**, *46*, 4085. (h) Lu, M.; Campbell, J. L.; Chauhan, R.; Grapperhaus, C. A.; Chen, H. *J. Am. Soc. Mass Spectrom.* **2013**, *24*, 502. (i) Chauhan, R.; Mashuta, M. S.; Grapperhaus, C. A. *Inorg. Chem.* **2012**, *51*, 7913.

(10) Frisch, M. J.; et al. *Gaussian 09*, revision B.01; Gaussian, Inc.: Wallingford, CT, 2013.

(11) Werner, H. J.; et al. *MOLPRO*, a package of ab initio programs, 2012; see http://www.molpro.net.

(12) Tedder, J. M. *Angew. Chem., Int. Ed. Engl.* **1982**, *21*, 401.

DOI: 10.1021/jacs.5b09309
J. Am. Chem. Soc. 2015, 137, 15616−15619